

PDR

EGG-SAAM-6415

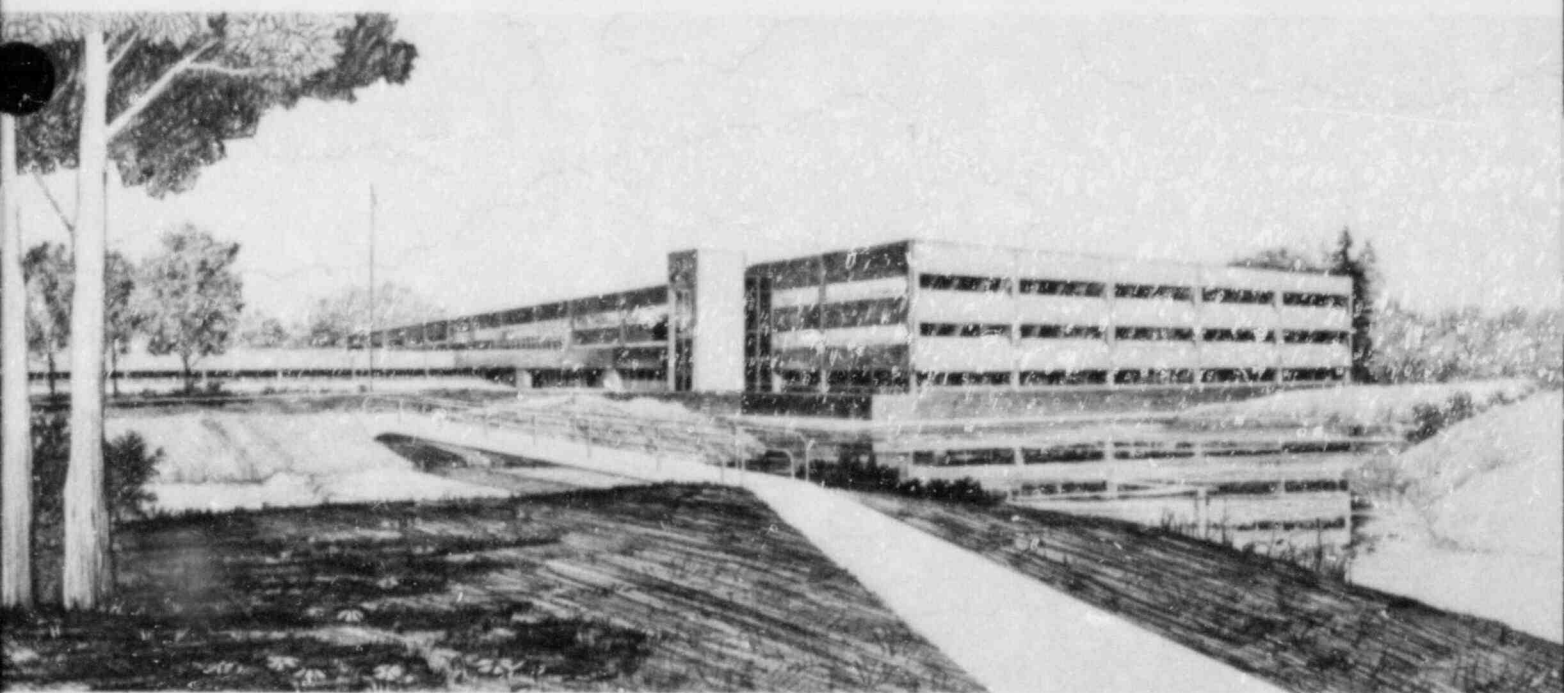
September 1983

ANALYSIS OF THE JANUARY 29, 1980 TURBINE TRIP
AT ARKANSAS NUCLEAR ONE UNIT 2

Paul D. Bayless

Idaho National Engineering Laboratory

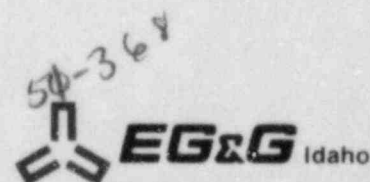
Operated by the U.S. Department of Energy



This is an informal report intended for use as a preliminary or working document

8403280124 830930
PDR ADOCK 05000368
S PDR

Prepared for the
U.S. NUCLEAR REGULATORY COMMISSION
Under DOE Contract No. DE-AC07-76ID01570
FIN No. A6234



ANALYSIS OF THE JANUARY 29, 1980 TURBINE TRIP
AT ARKANSAS NUCLEAR ONE UNIT 2

Paul D. Sayless

Published September 1983

EG&G Idaho, Inc.
Idaho Falls, Idaho 83415

Prepared for the
U.S. Nuclear Regulatory Commission
Washington, D.C. 20555
Under DOE Contract No. DE-AC07-76ID01570
FIN No. A6234

ABSTRACT

The turbine trip that occurred at Arkansas Nuclear One Unit 2 on January 29, 1980 was analyzed using the RELAP5 computer code. The transient was investigated to understand the overall plant response, particularly in relation to natural circulation cooling. Sensitivity calculations were performed to explain the transient response. Methods of identifying the presence of natural circulation cooling were investigated.

FIN No. A6234--Analytical Assessment of Reactor Operational Events

SUMMARY

An analysis of the January 29, 1980 turbine trip at Arkansas Nuclear One Unit 2 (ANO-2) was performed using the RELAP5 computer code. The analysis of the turbine trip transient was performed by EG&G Idaho, Inc., at the Idaho National Engineering Laboratory. This analysis was the fifth in a series of analyses requested by the Nuclear Regulatory Commission's Office for Analysis and Evaluation of Operational Data to support case studies of natural circulation events in PWRs. ANO-2 is a Combustion Engineering pressurized water reactor (PWR) with a rated core thermal power of 2815 MW. RELAP5 is an advanced computer code designed for one-dimensional, thermal-hydraulic analysis of nuclear reactor and related experimental systems.

The analysis was performed to provide an understanding of the overall plant response, with emphasis on natural circulation cooling. It was also intended to identify operator actions that may have been taken during the transient and to investigate their effect on natural circulation.

A base calculation was performed using only the known operator actions and component operations. This calculation represented the trends of the data fairly well. Additional calculations were performed to more accurately represent the plant behavior. These included investigations of the effects of the steam generator pressure, pressurizer level, high pressure safety injection flow, and reactor vessel upper head temperature.

Based on the analysis, it was concluded that no significant operator actions were taken that were not reported in the transient descriptions. It was concluded, however, that the emergency feedwater flow to one steam generator was reduced during the transient.

A stable natural circulation flow was established in each of the calculations that extended past the reactor coolant pump coastdown. The transition to and presence of natural circulation cooling in both the plant and the calculations could be inferred from temperature measurements. The cold leg temperature was closely coupled to the steam generator temperature during natural circulation. Also, the difference between the hot and cold leg temperatures increased during the transition from forced convection to natural circulation cooling, then stayed fairly constant in fully developed natural circulation flow.

CONTENTS

ABSTRACT	ii
SUMMARY	iii
1. INTRODUCTION	1
2. MODEL DESCRIPTION	3
2.1 Nodalization	3
2.2 Initial Conditions	9
2.3 Boundary Conditions	9
3. TRANSIENT ANALYSIS	12
3.1 Transient Investigation	12
3.2 Natural Circulation	29
4. CONCLUSIONS	33
5. REFERENCES	35

FIGURES

1. RELAP5 nodalization of ANO-2 coolant loops	4
2. RELAP5 nodalization of ANO-2 reactor vessel	5
3. RELAP5 nodalization of ANO-2 A steam generator	6
4. RELAP5 nodalization of ANO-2 B steam generator	7
5. RELAP5 nodalization of ANO-2 main steam lines	8
6. Pressurizer pressure from the base case and the plant data	14
7. Pressurizer liquid level from the base case and the plant data	14
8. Loop A hot leg temperature from the base case and the plant data	15

9.	Loop A cold leg temperatures from the base case and the plant data	15
10.	Steam generator A and B pressures from the base case and the plant data	16
11.	Steam generator A and B narrow range liquid levels from the base case and the plant data	16
12.	Pressurizer pressure from the controlled pressure case, the base case, and the plant data	21
13.	Pressurizer liquid level from the controlled pressure case, the base case, and the plant data	21
14.	Loop A hot leg temperature from the controlled pressure case, the base case, and the plant data	22
15.	Loop A cold leg temperature from the controlled pressure case, the base case, and the plant data	22
16.	Pressurizer pressure from the pressurizer level case, the controlled pressure case, and the plant data	24
17.	Pressurizer liquid level from the pressurizer level case, the controlled pressure case, and the plant data	24
18.	Loop A hot leg temperature from the pressurizer level case, the controlled pressure case, and the data	25
19.	Steam generator A and B narrow range liquid levels from the pressurizer level case and the data	25
20.	Pressurizer pressure from the higher pressure HPSI case, the pressurizer level case, and the data	28
21.	Pressurizer pressure from the hot upper head case, the pressurizer level case, and the data	28
22.	Hot leg mass flow rate from the base case and the pressurizer level case	30
23.	Loop temperature difference from the base case, the pressurizer level case, and the plant data	30
24.	Loop A cold leg and steam generator temperatures from the pressurizer level case	32
25.	Loop A cold leg and steam generator temperatures from the plant data	32

TABLES

1. Initial Conditions	10
2. Sequence of Events for the Turbine Trip Test	13

1. INTRODUCTION

The turbine trip that occurred at Arkansas Nuclear One Unit 2 (ANO-2) on January 29, 1980 was analyzed. The principal analysis tool used was the RELAP5 computer code. The analysis was performed in support of pressurized water reactor (PWR) natural circulation case studies being performed by the Nuclear Regulatory Commission's Office for Analysis and Evaluation of Operational Data. The objectives of the analysis were to understand the plant response during the transient, to identify possible operator actions that would account for the plant response, and to investigate natural circulation phenomena.

ANO-2 is a Combustion Engineering PWR with a rated core power of 2815 MW(t). On January 29, 1980 it was operating at 98% power when a turbine trip test was initiated. As the primary and secondary system pressures increased, the turbine bypass valves, one atmospheric dump valve (ADV), and one pressurizer spray valve opened. Decreasing liquid level in the steam generators caused a reactor scram and initiated emergency feedwater (EFW) injection. As the pressures decreased, the valves listed above were signaled to close, but the spray valve and the ADV stuck open. The stuck open valves caused a continued depressurization of the primary and secondary coolant systems. The pressure decreased far enough to allow the high pressure safety injection (HPSI) system to inject liquid into the primary coolant system. The reactor coolant pumps (RCPs) were tripped manually because the plant behavior was indicative of a small break loss of coolant accident. This action stopped the pressurizer spray. The main steam isolation valves (MSIVs) closed on a low steam generator pressure trip, isolating the open ADV. The pressures then began to recover.

RELAP5¹⁻⁸ is an advanced computer code designed for best estimate thermal-hydraulic analysis of postulated light water reactor transients. It is a one-dimensional analysis code based on a nonhomogeneous, nonequilibrium hydrodynamic model that utilizes one energy, two momentum, and two continuity equations. The versions of the code used in this analysis were RELAP5/MOD1.6 cycles 12, 13, and 14, which have been stored

under Configuration Control Numbers F01245, F01261, and F01277, respectively, at the Computer Science Laboratory at the Idaho National Engineering Laboratory.

The data presented in this report were digitized from plots presented in "NSSS Transient Tests at ANO-2".⁹ The quality of the measured data was not known. Some of the plots had noticeable offsets, so the data trends were considered more important than the magnitudes. The uncertainties in the time scales of the data presented in this report were estimated to be ≤ 1 s for the first 60 s, and ≤ 30 s thereafter.

This report is the fifth in a series of analyses of natural circulation events in PWRs. Previous analyses investigated loss of off-site power transients at ANO-2¹⁰ and ANO-1¹¹, a reactor coolant pump trip at McGuire,¹² and a natural circulation test at North Anna.¹²

A description of the RELAP5 model of ANO-2, including the initial and boundary conditions, is presented in Section 2. Results of the analysis of the turbine trip are presented in Section 3. Conclusions drawn from the analysis are presented in Section 4. References are presented in Section 5.

2. MODEL DESCRIPTION

The RELAP5 nodalization of ANO-2 used in the analysis is described in Section 2.1. The initial conditions are described in Section 2.2, and the boundary conditions are discussed in Section 2.3.

2.1 Nodalization

The RELAP5 model of ANO-2 consisted of 207 volumes, 215 junctions, and 171 heat structures. Nodalization diagrams for various parts of the plant are presented in Figures 1 through 5. The hydrodynamic components were modeled to represent the actual flow areas, lengths, volumes, and elevation changes that exist in the plant. The heat structures were modeled to represent the actual stored energy and heat transfer area of the metal components of the plant.

The nodalization of the coolant loops is shown in Figure 1. Both loops in the plant were modeled with each containing one hot leg, one steam generator, two cold legs, and two reactor coolant pumps. The pressurizer was connected to the A loop hot leg. The pressurizer model included the heaters, the surge line, and the main spray line. Flow from the HPSI pumps was injected into each cold leg. Charging flow was injected into one cold leg in each loop, and letdown was taken from one of the pump suction legs. Control systems were provided to operate the charging, letdown, and pressurizer heaters as they are operated in the plant. The charging and letdown were controlled by the deviation from the pressurizer setpoint level, which was determined by the loop average temperature. The proportional heater power varied linearly from full power at 15.34 MPa (2225 psia) to zero at 15.69 MPa (2275 psia).

The nodalization of the reactor vessel is shown in Figure 2. The reactor vessel was modeled to include the downcomer, lower plenum, core, upper plenum, upper head, core bypass flow paths, internals, and fuel rods. The modeled core bypass flow paths included the outlet nozzle clearances, the alignment key-ways, the support cylinder holes, the core

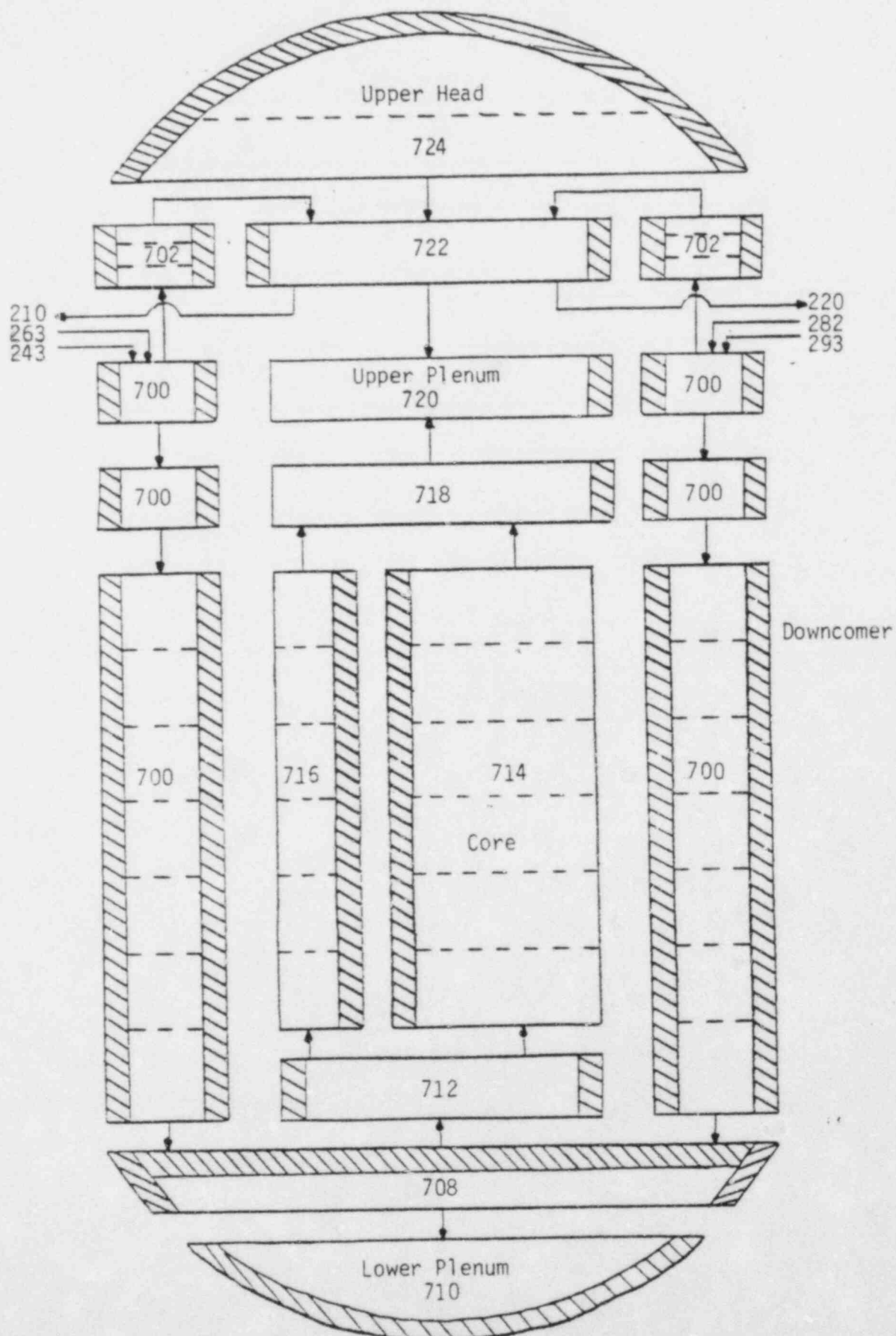


Figure 2. RELAP5 nodalization of ANO-2 reactor vessel.

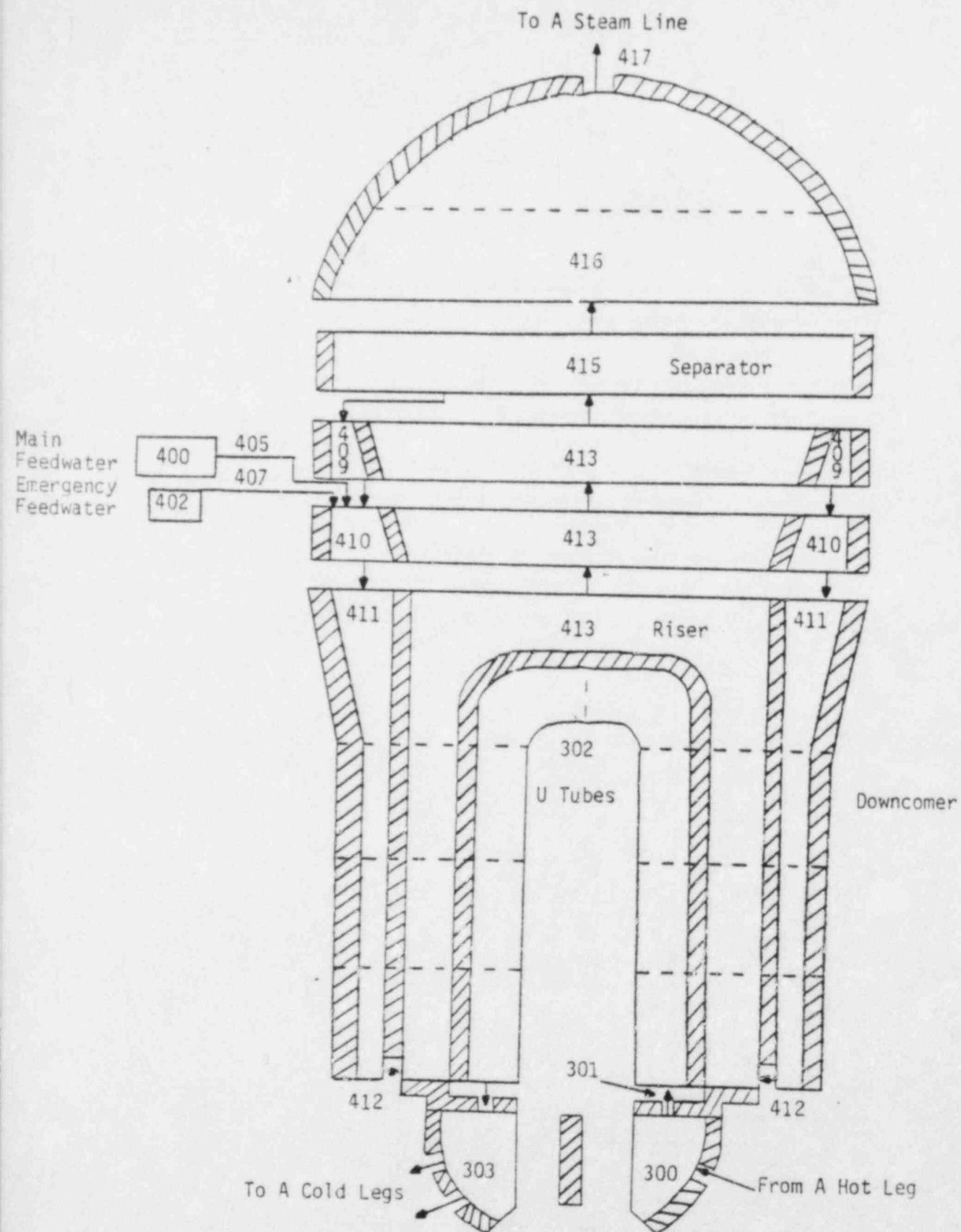


Figure 3. RELAP5 nodalization of ANO-2 A steam generator.

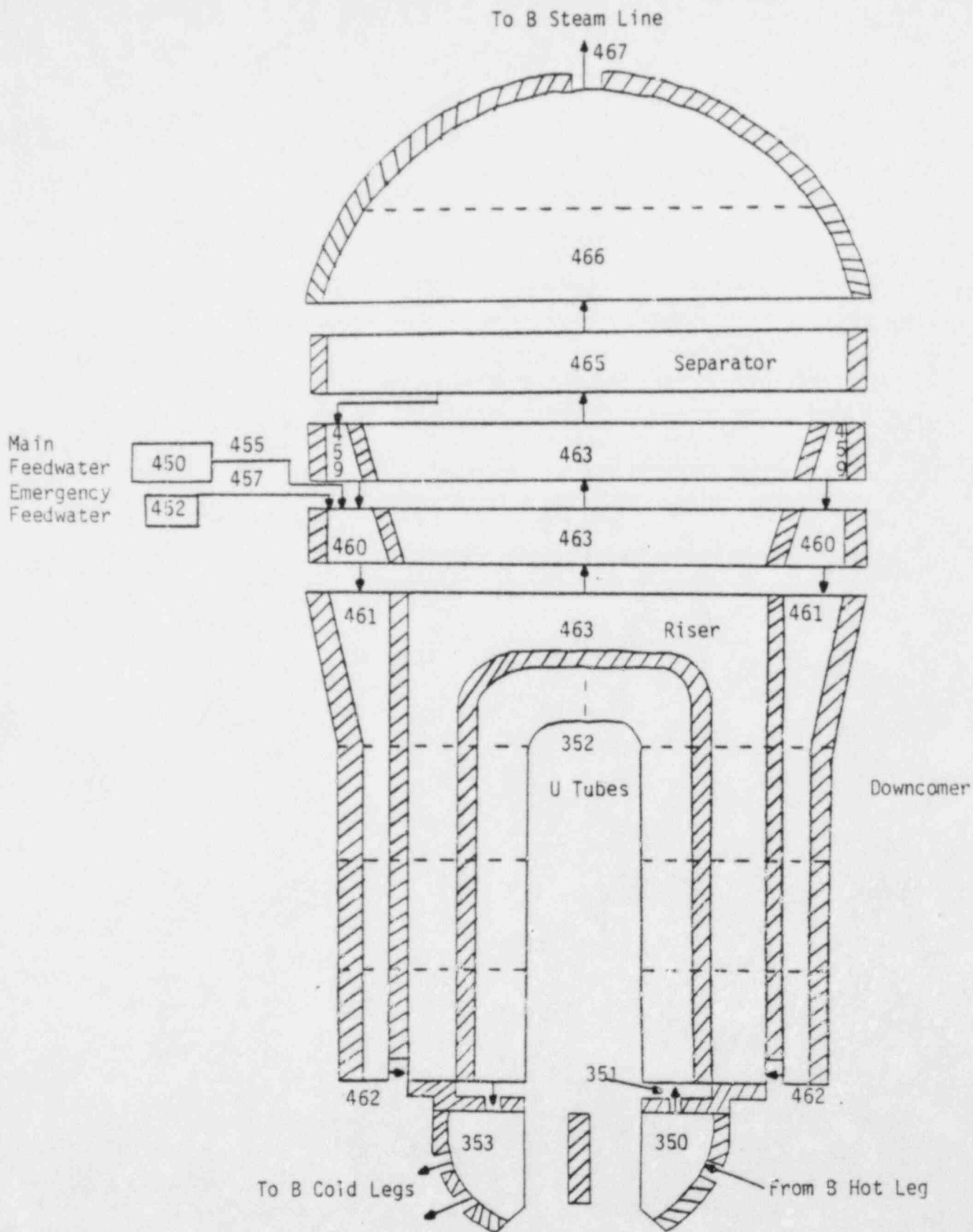


Figure 4. RELAP5 nodalization of ANO-2 B steam generator.

A MAIN STEAM LINE

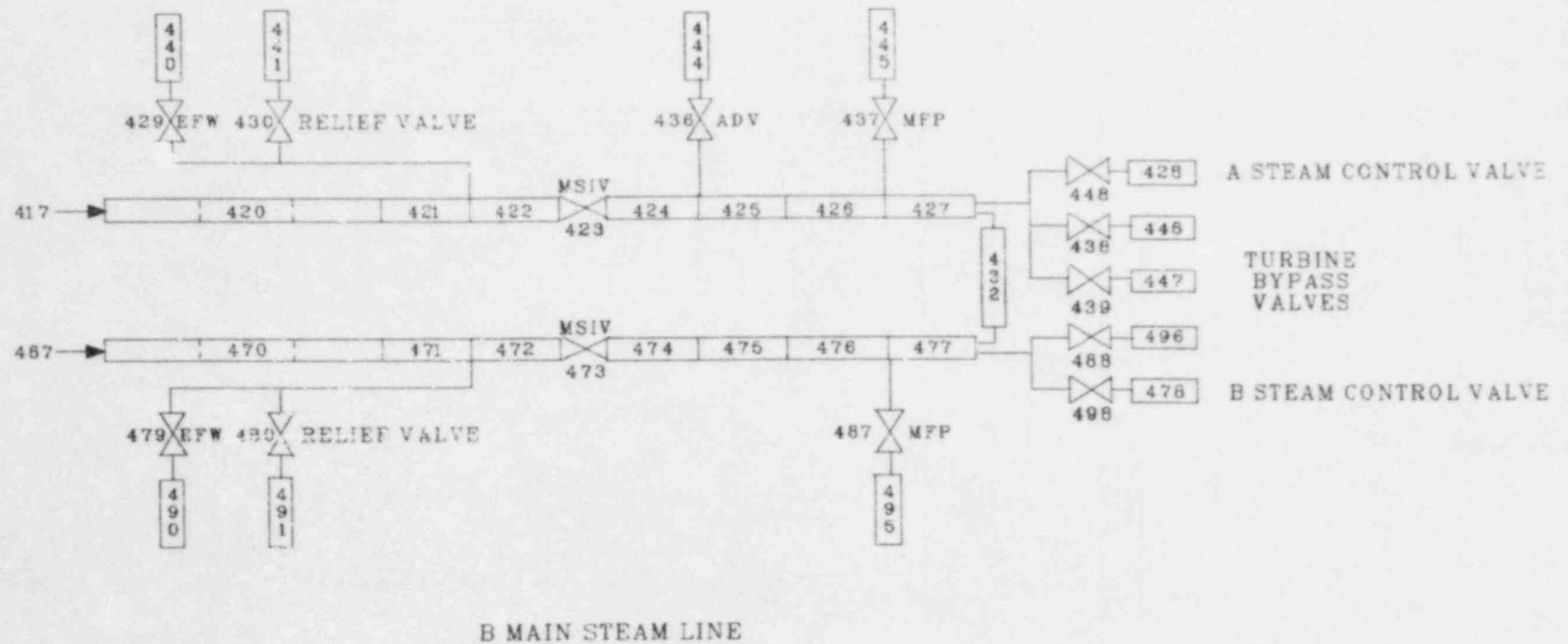


Figure 5. RELAP5 nodalization of ANO-2 main steam lines.

shroud clearances, and the guide tubes. The outlet nozzle clearance and alignment key-ways paths were lumped together and connected the inlet annulus to the upper plenum. The support cylinder holes, core shroud clearance paths and guide tubes were lumped together as a flow path parallel to but separate from the core. The portion of the guide tube bypass from the lower plenum to the upper head was not modeled explicitly.

Figures 3 through 5 present the nodalization of the secondary coolant system. The main and emergency feedwater connections to the steam generators were modeled. The main steam lines were modeled from the steam generators to the main steam control valves. Connections to the steam lines included steam supply lines to the main and emergency feedwater pump turbines, the four available steam dump and bypass valves, the lowest pressure relief valves, and a cross-tie between the main steam lines.

2.2 Initial Conditions

The initial conditions used in the RELAP5 calculations are compared to the actual transient initial conditions in Table 1. The plant initial conditions were obtained from Reference 9. The RELAP5 initial values were obtained from a steady state calculation in which the reactor coolant pumps, chemical and volume control system, and feedwater and steam flows were operated by control systems. The agreement between the calculated and actual values was generally excellent. The difference in the reactor coolant flow was not considered significant because the measured flow rate was inconsistent with the power and the hot and cold leg temperatures.

2.3 Boundary Conditions

The boundary conditions described below are those that were assumed for the RELAP5 calculations.

At transient initiation, the steam control valves began to close, simulating a one-second closing of the turbine stop valves, and a one-second feedwater coastdown was initiated, simulating the closing of the

TABLE 1. INITIAL CONDITIONS

Parameter	RELAP5	Plant
Core power, MW	2764	2764
Pressurizer pressure, MPa (psia)	15.55 (2256)	15.55 (2256)
Hot leg temperature, K (°F)	594.5 (610.4)	594 (610)
Cold leg temperature, K (°F)	562.0 (552.0)	562 (552)
Pressurizer level, %	49.4	49.2
Reactor coolant flow, kg/s (lbm/s)	15,190 (33,490)	16,760 (36,950)
Charging flow, l/s (gpm)	2.52 (39.9)	2.85 (45.2)
Letdown flow, l/s (gpm)	2.48 (39.4)	2.55 (40.4)
Boron concentration, ppm	599	599
Steam generator pressure, MPa (psia)	6.25 (907)	6.26 (908)
Steam generator narrow range liquid level, %	73	72
Steam flow, kg/s (lbm/s)	767 (1690)	815 (1800)
Feedwater flow, kg/s (lbm/s)	767 (1690)	787 (1740)

feedwater control valves. At 2 s, the steam dump and bypass valves were opened, as were the pressurizer spray valves. The reactor was scrammed and the EFW injection started at 6.1 s. The EFW system provided 36.3 l/s (575 gpm) of 304 K (88°F) water to each steam generator.

At 24.5 s, the turbine bypass valves and one pressurizer spray valve were closed. The ADV remained full open, and one pressurizer spray valve remained half open. It was not known how far open the spray valve actually remained. The RCPs were tripped between 200 and 204 s. The safety injection actuation signal (SIAS) was reset at 700 s.

The core power was calculated using the point kinetics available in RELAP5. The power history prior to the transient initiation was obtained from Reference 13. Reactivity coefficients and weighting factors were obtained from References 14 and 15, and were based on a fuel burnup of 3200 MWD/MTU.

3. TRANSIENT ANALYSIS

Results of the evaluation of the plant thermal-hydraulic response during the transient are presented in Section 3.1. An analysis of how the various conditions simulated in the sensitivity studies affected natural circulation and of how natural circulation might be identified is presented in Section 3.2.

3.1 Transient Investigation

The sequence of events for the turbine trip test is presented in Table 2. The information for the table was obtained from References 9 and 16.

A base calculation was performed using only the boundary conditions described in Section 2.3. Major parameters from this calculation are compared with the plant data in Figures 6 through 11.

Figure 6 presents the pressurizer pressure comparison. The pressure increased following the turbine trip because the steam generators were not removing as much energy from the reactor coolant system (RCS) as before and the core power remained high. This caused a temperature increase in the RCS liquid, decreasing its density and increasing the liquid volume, which compressed the steam in the pressurizer and raised the pressure. The calculated pressurization rate decreased at 2 s as the pressurizer spray began condensing steam. The pressure began to decrease at 8 s, shortly after the reactor scram (6.1 s). As the power decreased following the scram, the steam generators began removing more energy from the RCS than the core was putting in, reducing the liquid temperature and reversing the process that caused the initial pressurization. The depressurization rate decreased between 25 and 30 s because the turbine bypass valves closed, reducing the energy removal through the steam generators, and because a pressurizer spray valve closed, reducing the steam condensation in the pressurizer. The depressurization rate increased near 170 s in the calculation (125 s in the data) as steam from the pressurizer began entering the hot leg. The pressure decreased more rapidly because there was no saturated liquid remaining that could flash to steam as

TABLE 2. SEQUENCE OF EVENTS FOR THE TURBINE TRIP TEST

Time (s)	Event
0.0	Main turbine tripped
2.0	Turbine bypass valves, ADV, pressurizer spray valve signaled to open
6.1	Reactor scram; emergency feedwater actuation signal generated
21	Turbine bypass valves, ADV, pressurizer spray valve signaled to close
29	Turbine bypass valves closed
102.6	SIAS
144	Pressurizer emptied
200	RCP B tripped
202	RCPs A and C tripped
204	RCP D tripped
241.5	Main steam isolation signal
274	ADV closed manually
303	Pressurizer level on-scale
~700	Reset SIAS

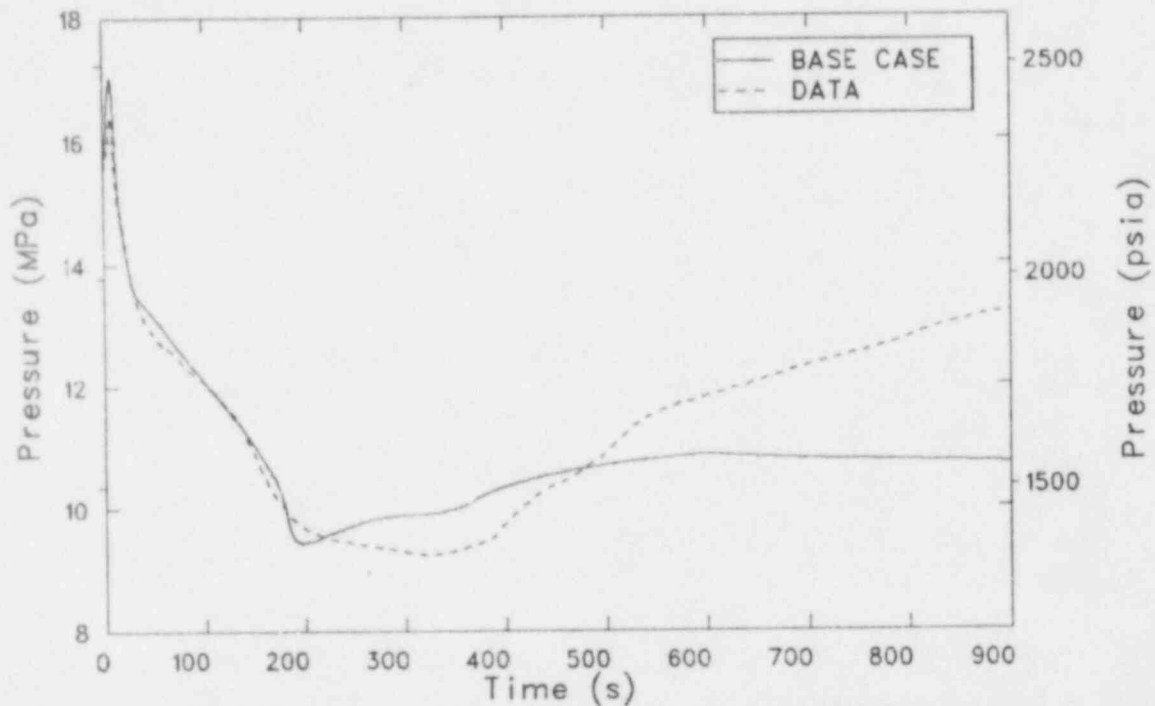


Figure 6. Pressurizer pressure from the base case and the plant data.

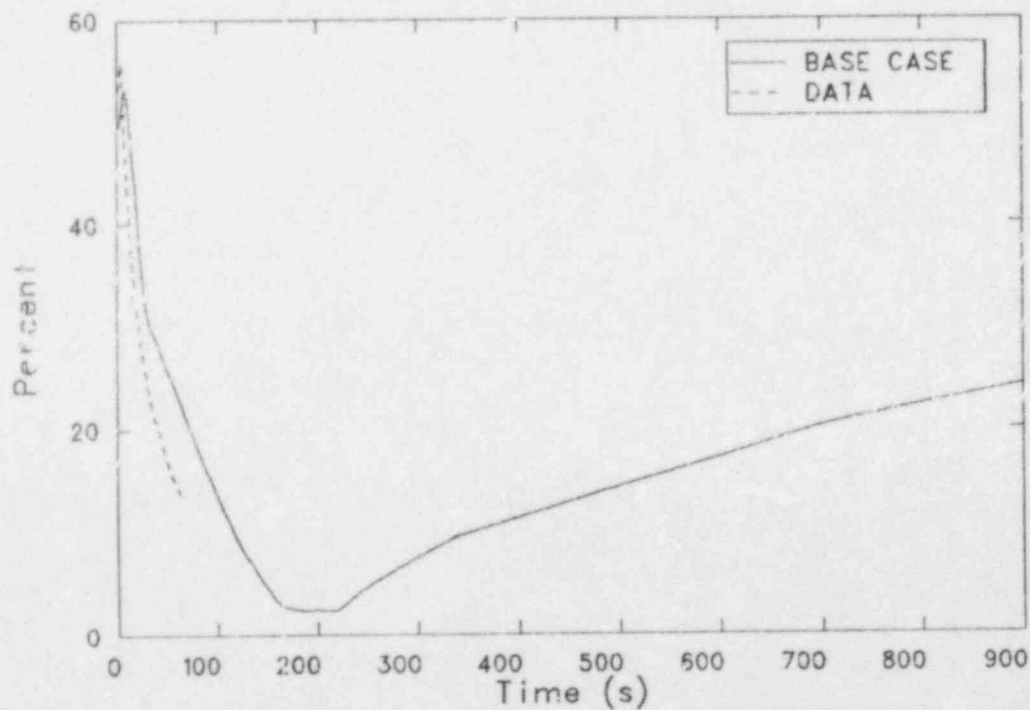


Figure 7. Pressurizer liquid level from the base case and the plant data.

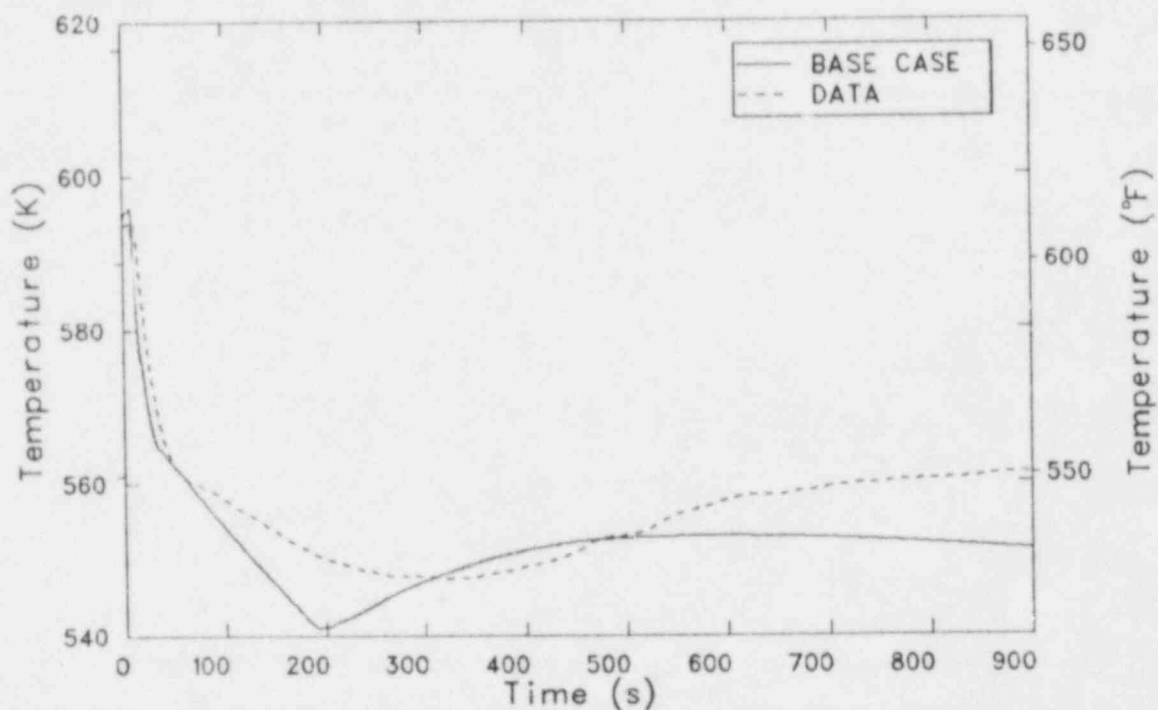


Figure 8. Loop A hot leg temperature from the base case and the plant data.

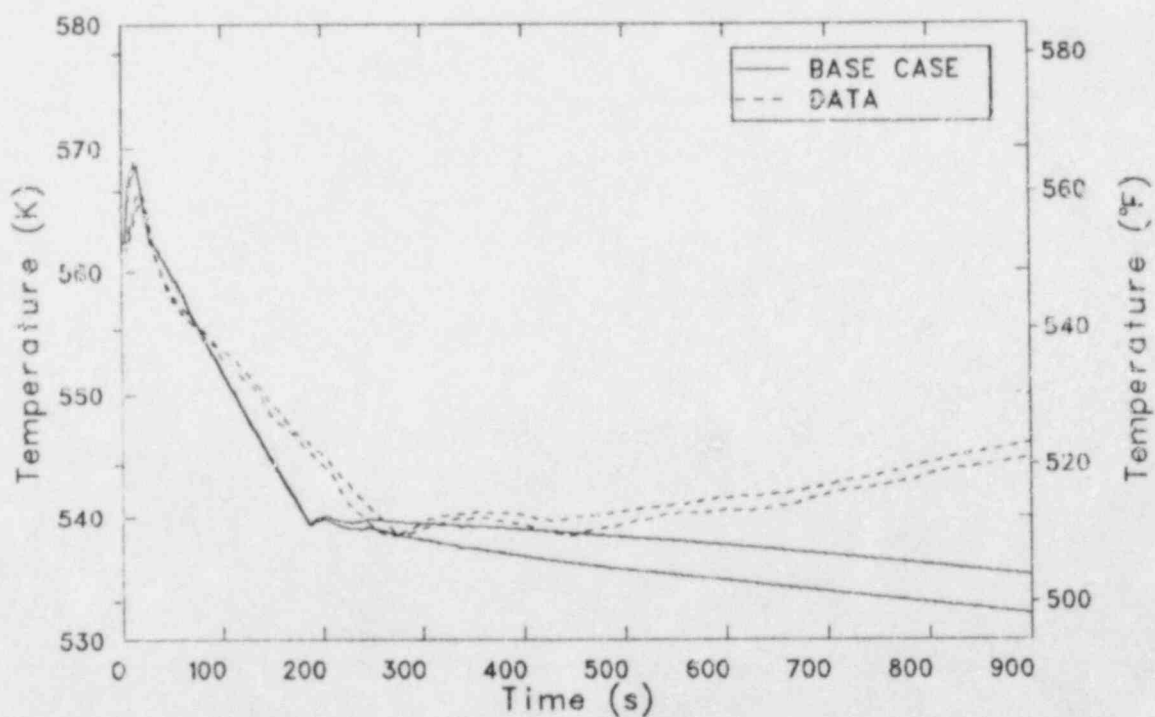


Figure 9. Loop A cold leg temperatures from the base case and the plant data.

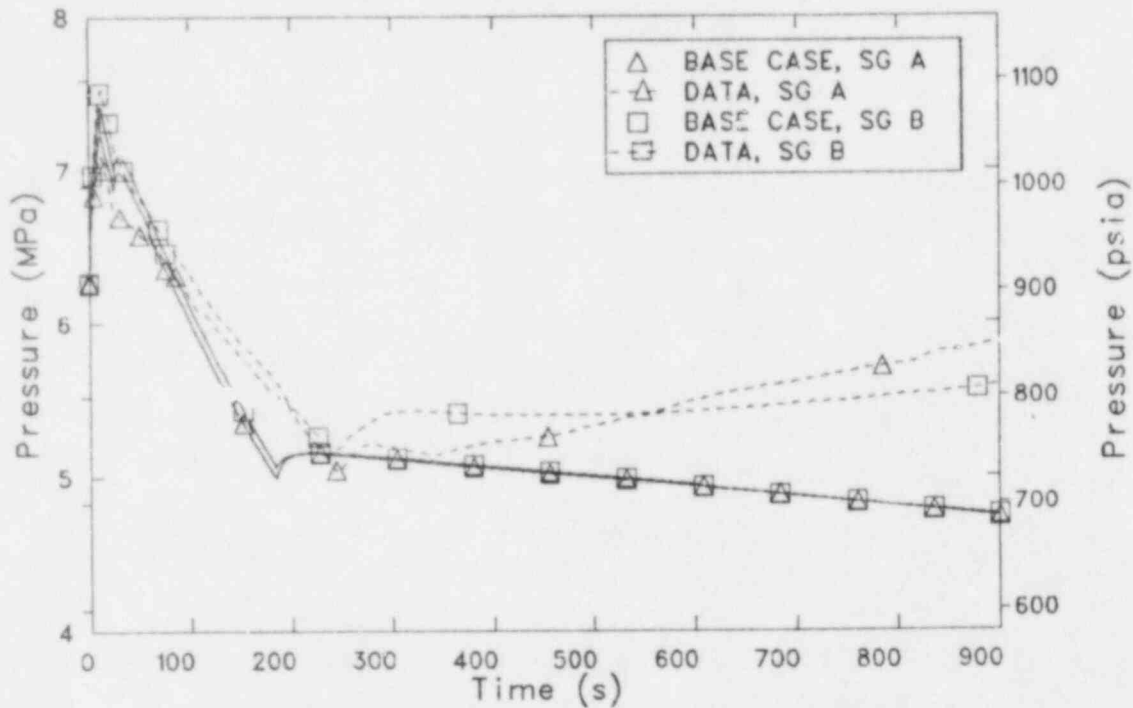


Figure 10. Steam generator A and B pressures from the base case and the plant data.

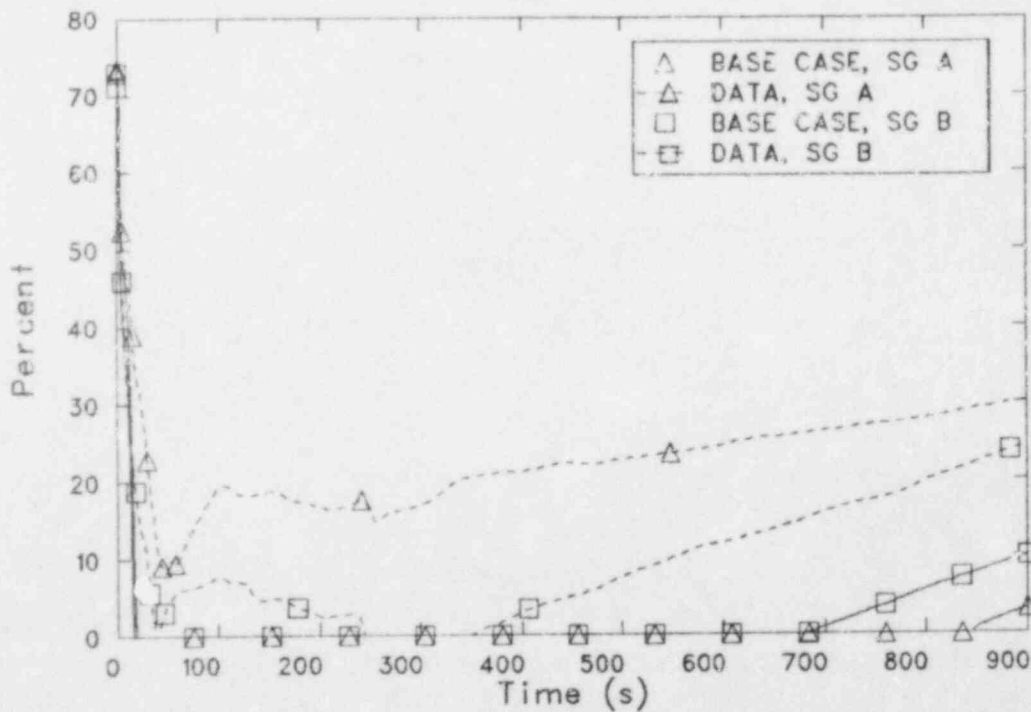


Figure 11. Steam generator A and B narrow range liquid levels from the base case and the plant data.

the pressure dropped, and because the steam that entered the hot leg was quickly condensed by the subcooled liquid in the piping, thus reducing the total amount of steam. The calculated depressurization stopped shortly after the MSIVs closed near 185 s. The steam flow from the steam generators decreased because the open ADV was isolated from the steam generators, so the energy removal from the RCS decreased. Also at 185 s, the pressure had dropped far enough that HPSI began. The reactor coolant pressure began to increase after the RCPs were tripped around 200 s. As the flow coasted down, the liquid passing through the core was heated more, which in turn caused the RCS to heat up and pressurize. Also, the pressurizer spray through the stuck open spray valve was eliminated when the pumps were tripped. The pressure leveled off after about 600 s because the insurge of cooler liquid from the hot leg to the pressurizer condensed sufficient steam to balance the compression of the vapor.

The calculated pressure trends and values agreed very well with the data until the MSIVs closed. The data did not show sharp slope changes when the MSIVs closed or when the pumps were tripped. The difference in trend after 600 s was primarily caused by an excessive condensation rate in the calculation during the insurge to the pressurizer.

The pressurizer level comparison is shown in Figure 7. No level data were available after about 65 s. The level increased following the turbine trip as the liquid in the RCS heated and expanded. The level began to decrease after the reactor scrammed because the RCS liquid was cooling. The rate of the level decrease dropped around 30 s in both the calculation and the data because the turbine bypass valves closed, slowing the cooldown of the RCS. In the calculation, the level remained nearly constant between 170 and 220 s because mostly steam was being drawn through the surge line to the hot leg. The level did not decrease to 0.0 because the pressurizer was modeled such that there was a stagnant volume below the surge line connection to the pressurizer. This volume remained filled with liquid through most of the transient. The level then began to increase because of injection from the charging and HPSI pumps and increasing RCS temperature. The slope change at about 340 s was caused by a change in the calculated

condensation rate. The level continued to increase as the three charging pumps kept injecting liquid into the system. At 700 s the SIAS was reset, allowing the letdown flow to be reinstated, and the level increase slowed.

The hot leg temperatures are compared in Figure 8. The calculated hot leg temperature increased after the turbine trip because the steam generators were removing less energy from the RCS than the core was adding. This condition was reversed after the reactor scram, and the temperature decreased. The decrease was slowed around 30 s in both the data and the calculation when the turbine bypass valves closed, reducing the energy removal through the steam generators. The calculated temperature leveled off when the MSIVs closed near 185 s, and increased after the RCPs were tripped around 200 s. The flow coastdown caused the fluid passing through the core to be heated more. The temperature rose more slowly and then decreased after about 500 s as natural circulation flow was established and the steam generators cooled the RCS. The measured temperature did not have sharp changes in slope when the pumps were tripped near 200 s or when the MSIVs closed near 240 s. The difference in trend after about 400 s was caused by differences in the calculated and measured steam generator behavior that will be discussed later.

Figure 9 presents a comparison of the temperatures from both cold legs in the A loop. The cold leg temperature increased in the calculation and the data as the RCS heated up following the turbine trip. The temperatures decreased after the reactor scrammed at 6.1 s. The temperatures then followed the steam generator secondary temperature, because the reactor power was low enough and the loop flow high enough to cool the reactor coolant nearly to the steam generator temperature as it flowed through the steam generator tubes in both forced and natural circulation flow. The calculated temperature decreased until the MSIVs closed, then remained nearly constant for 50 to 100 s before decreasing again. The differences between the calculated and measured temperatures were caused by differences in the steam generator behavior that will be discussed later. The difference between the two calculated temperatures after about 200 s was caused by the charging flow. Charging flow entered one cold leg in each loop, and the cold leg temperature measurement was located downstream of the injection location.

The pressures from both steam generators are compared in Figure 10. The closing of the turbine stop valves caused a rapid increase in pressure as the transient began. This increase was slowed by the opening of the turbine bypass and atmospheric dump valves at 2 s. At 6.1 s, the reactor scrammed, reducing the heat input from the RCS, and the EFW injection began, condensing some of the steam in the steam generators. The pressure peaked around 12 s, then began to decrease because the steam release and condensation rates were greater than the boiling rate around the tubes. The calculated pressure increased briefly after the turbine bypass valves closed around 25 s, then began to decrease again. The measured depressurization rate decreased significantly when the bypass valves closed. Both pressures continued to decrease until the MSIVs closed. The higher depressurization rate in the calculation was caused by a higher steam flow through the open ADV. After the MSIVs closed, the pressure increased until the heat transfer from the RCS decreased so that the vapor generation rate was offset by the condensation rate. The pressures then decreased because the EFW condensed more steam than the heat input from the RCS could generate. The change in slope in the A steam generator data near 340 s may have been caused by a reduction in the EFW flow rate, which would have reduced the condensation rate. The increase in the measured B steam generator pressure after about 500 s was caused by increased heat transfer from the RCS as it heated up. The increasing pressure trend and the associated increasing RCS temperature was not seen in the calculation because the EFW flow to the two steam generators was high enough to remove all of the decay heat.

Figure 11 presents a comparison of the narrow range liquid levels for both steam generators. The calculated levels remained off scale for most of the transient, indicating that the initial steam generator liquid masses were different in the calculation and in the plant, that there were differences in the mass distribution in the steam generators between the plant and the calculation during the transient, or that the main feedwater coastdown was not as rapid as was assumed. Since the measured level in steam generator A did not go off scale, while that in steam generator B did, it appeared that more feedwater was delivered to steam generator A than to B in the first 50 s of the transient. This was confirmed by the

feedwater flow data. The rates of the calculated level increases after 650 s indicated that the EFW flow rate into steam generator B was good, but that the flow into steam generator A was too high. This latter observation, together with the change in the rate of the A steam generator measured level increase near 340 s, were further indications of a reduction in EFW flow to the A steam generator around 340 s.

In general, the calculated trends agreed very well with the data until the MSIVs closed. After the MSIVs closed, the differences in trend were primarily caused by differences in the steam generator behavior. The faster depressurization of the steam generator in the calculation resulted in the MSIVs closing before the RCPs were tripped, whereas in the actual transient the MSIVs closed after the pump trip.

In order to determine if there were any phenomena occurring in the RCS that were being masked by the differences in steam generator behavior, a calculation was performed in which the steam generator pressures were controlled to match the data. Also, the pressurizer spray valve was assumed to be stuck full open to compensate the slower RCS depressurization expected with the slower steam generator depressurization. Figures 12 through 15 present comparisons of the results of this calculation with the base calculation and the data.

The pressurizer pressures are compared in Figure 12. The controlled pressure calculation and the data were in excellent agreement until about 125 s. At that time, the data responded to the emptying of the pressurizer, while in the calculation the pressurizer level remained high enough that no steam was drawn into the surge line. In the controlled pressure calculation, the depressurization rate slowed after the RCPs were tripped around 200 s because the lower flow rate resulted in an increasing hot leg temperature. The pressure began to increase after the MSIVs closed because the RCS liquid was heating up and expanding. The steady pressure between 300 and 360 s was the result of excessive condensation in the pressurizer and was not realistic. The pressure increase after 360 s was not reasonable (in light of the pressurizer level response) and was caused by a problem in RELAP5 that began when subcooled liquid was introduced to a volume filled with superheated steam.

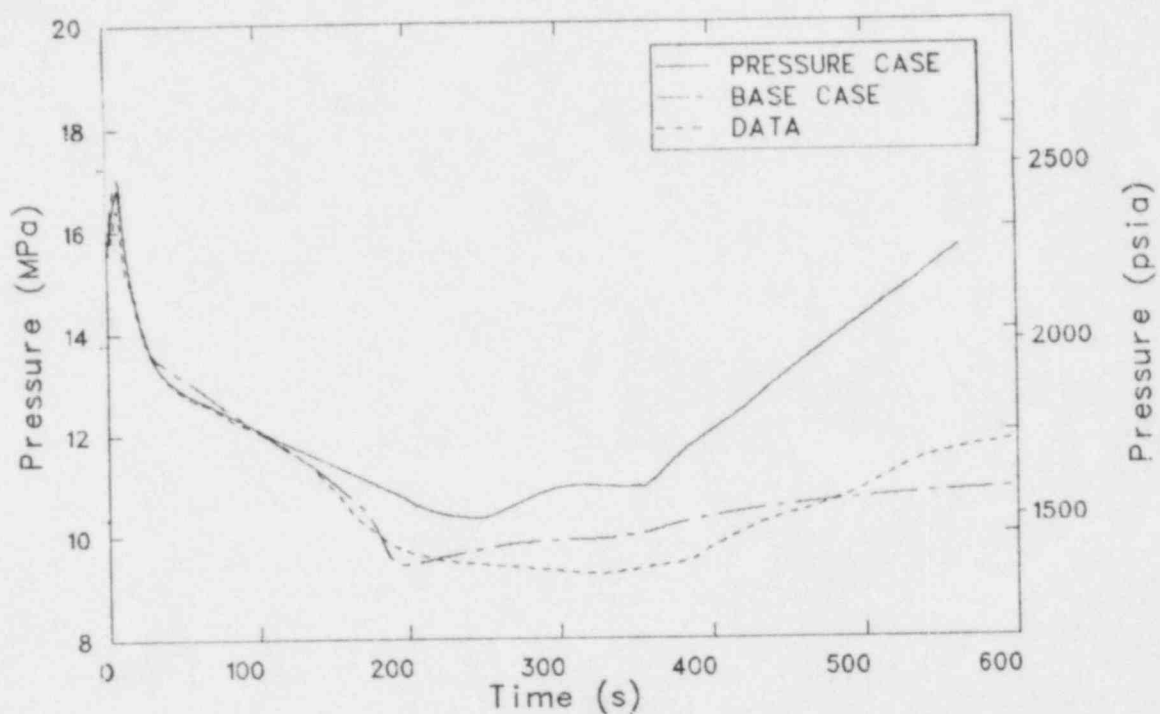


Figure 12. Pressurizer pressure from the controlled pressure case, the base case, and the plant data.

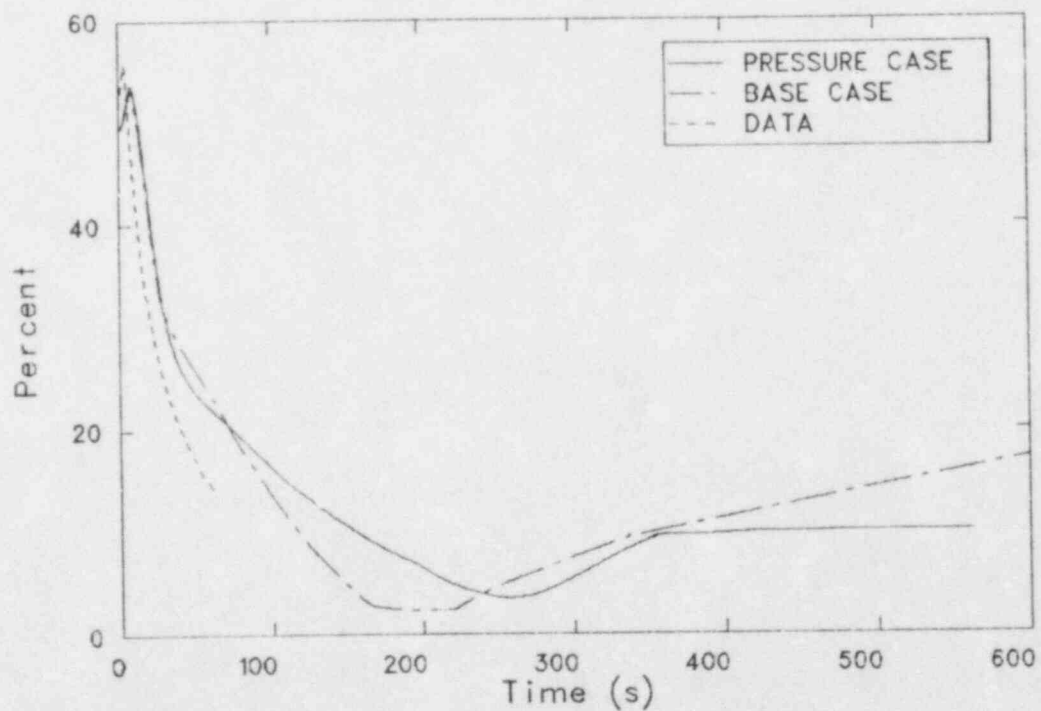


Figure 13. Pressurizer liquid level from the controlled pressure case, the base case, and the plant data.

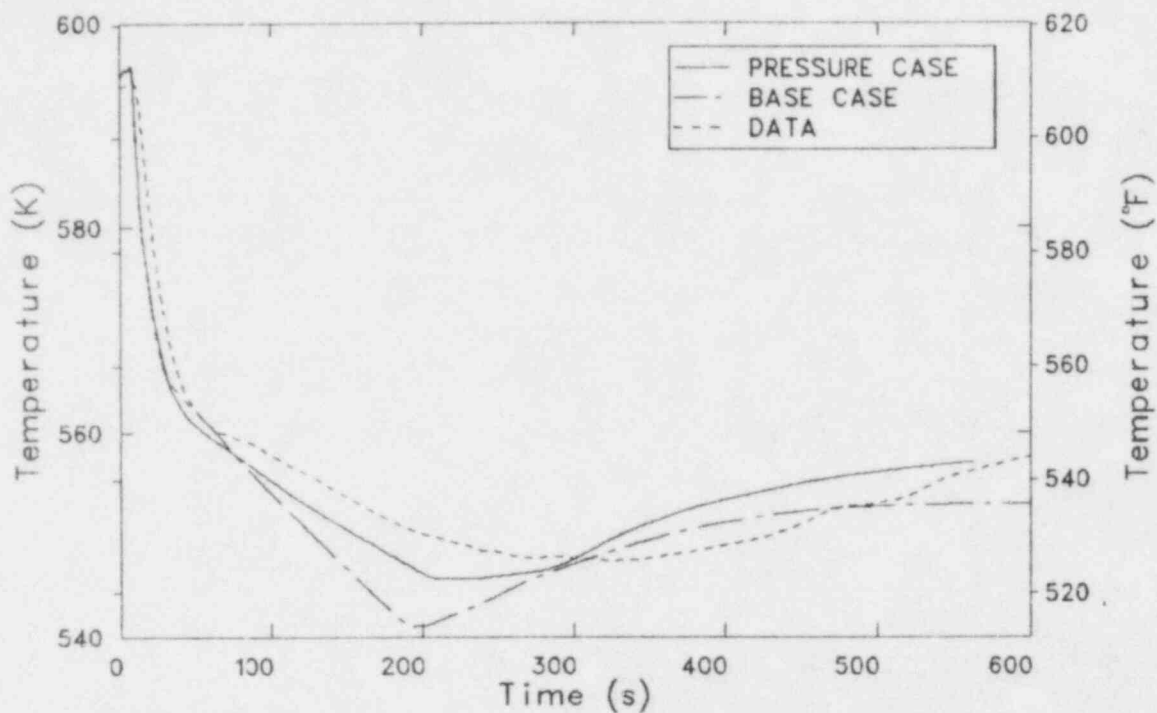


Figure 14. Loop A hot leg temperature from the controlled pressure case, the base case, and the plant data.

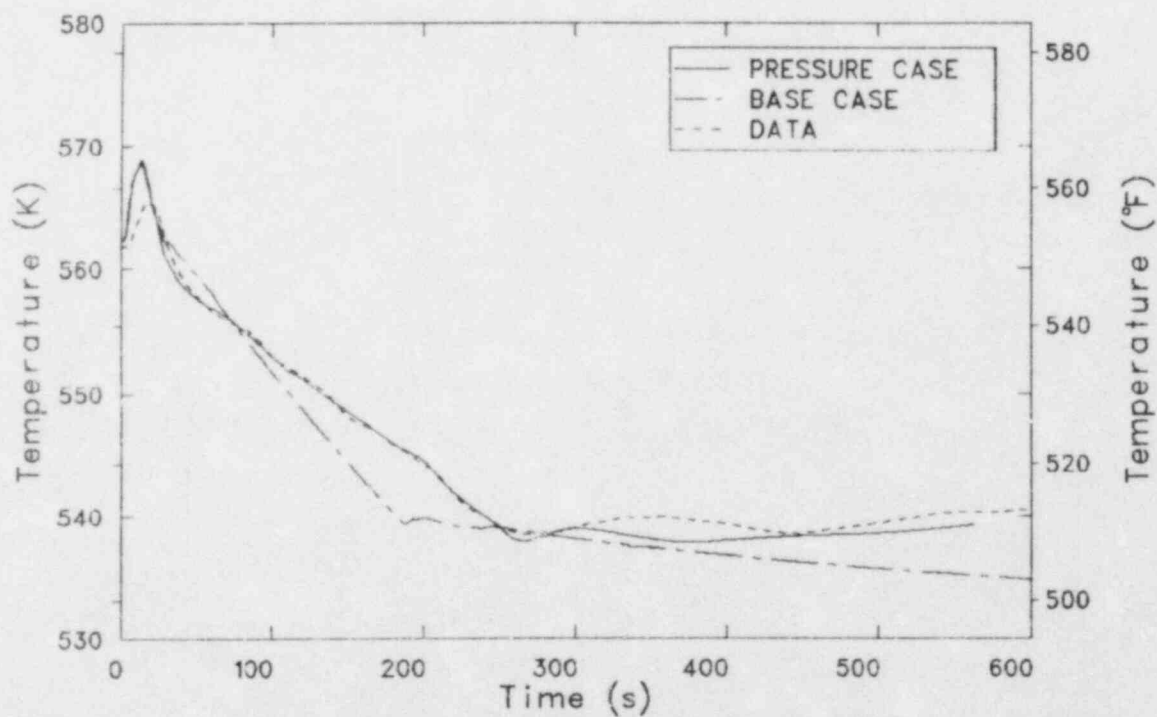


Figure 15. Loop A cold leg temperature from the controlled pressure case, the base case, and the plant data.

Figure 13 presents the pressurizer level comparison. As in the base calculation, the rate of the level decrease slowed after the turbine bypass valves closed near 25 s. The level continued to decrease as the RCS cooled until after the MSIVs closed near 245 s. However, the level did not decrease far enough to allow steam to be drawn from the pressurizer to the hot leg. The level began to increase after the MSIVs closed because the reactor coolant began to heat up. The constant level after 360 s was not realistic, and was caused by the same code problem that caused the pressure increase during this time.

The hot leg temperature comparison is shown in Figure 14. The slope of the temperature in the controlled pressure calculation agreed much more closely with the data during the first 200 s than did the base calculation temperature. The calculated temperature decrease stopped when the RCPs were tripped. The temperature slowly increased as the pumps coasted down, with the rate increasing after the MSIVs closed.

The cold leg temperatures from the A loop are compared in Figure 15. The measured and calculated cold leg temperatures were in excellent agreement. This was expected because the steam generator pressure was controlled to the data, and after the reactor scram the cold leg temperatures were very close to the steam generator secondary temperatures in both forced and natural circulation cooling.

The controlled pressure calculation agreed fairly well with the RCS data, except for the pressure response associated with the apparent emptying of the pressurizer. Since the calculated and measured temperatures were in good agreement, the amount of coolant shrink was not believed to have been responsible for the difference. To get a better pressure response, a calculation was performed in which the initial pressurizer level was reduced to 35%, with the steam generator pressures still controlled to the data. The level was reduced to 35% so that the pressurizer would empty at approximately the same time that the depressurization rate increased in the data. The results of this calculation are compared with the controlled pressure calculation and the data in Figures 16 through 19.

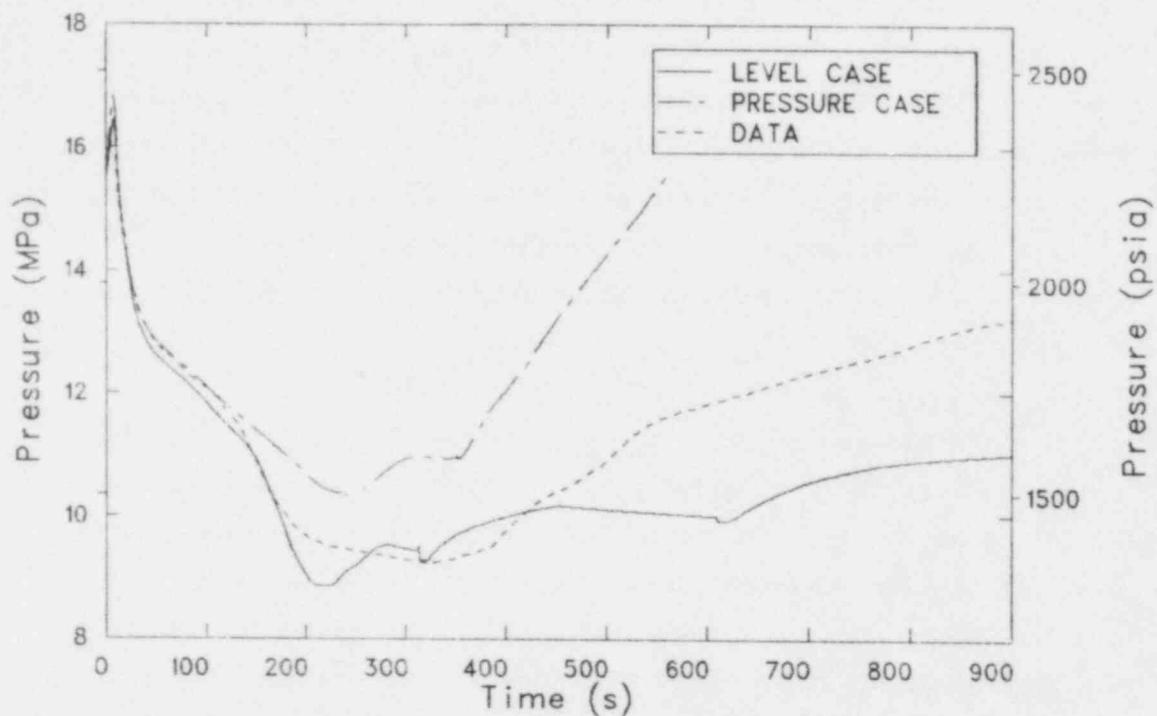


Figure 16. Pressurizer pressure from the pressurizer level case, the controlled pressure case, and the plant data.

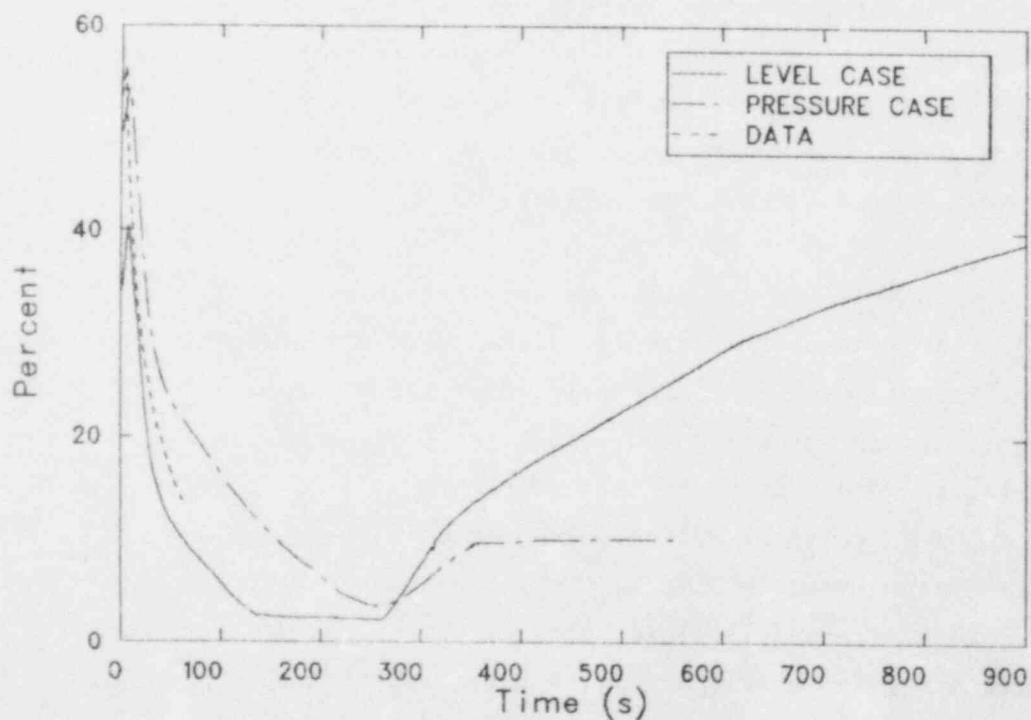


Figure 17. Pressurizer liquid level from the pressurizer level case, the controlled pressure case, and the plant data.

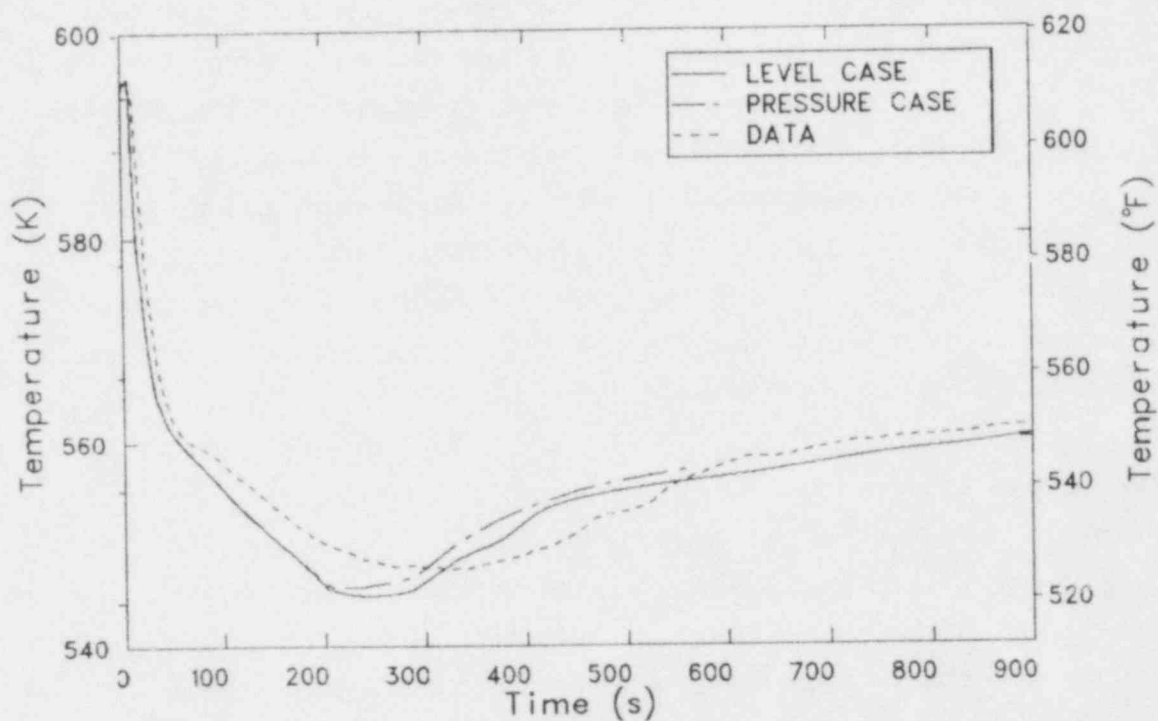


Figure 18. Loop A hot leg temperature from the pressurizer level case, the controlled pressure case, and the data.

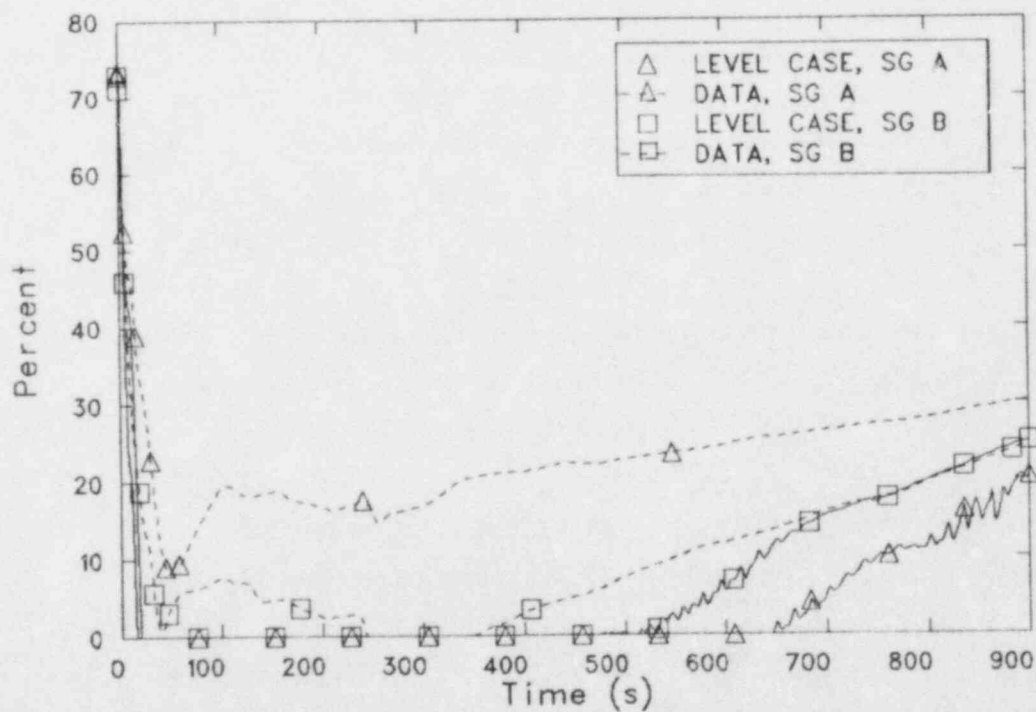


Figure 19. Steam generator A and B narrow range liquid levels from the pressurizer level case and the data.

Figure 16 presents the pressurizer pressure comparison. As expected, the pressure trends were more closely matched between 100 and 200 s. In the pressurizer level calculation the rapid depressurization stopped at about 210 s, or 6 s after the last RCP was tripped, whereas in the data the depressurization rate had decreased before the pumps were tripped. The overall trend in the calculation after 250 s was to increase the pressure as the RCS heated up, but the calculated condensation rate in the pressurizer during the insurge was too high. The decreases in pressure near 315 and 610 s occurred when volumes in the modeled pressurizer filled with liquid, and were not realistic.

The pressurizer level comparison is presented in Figure 17. Steam started to flow from the pressurizer at about 130 s, and the level did not begin to increase until about 260 s. The changes in the rate of the level increase at 315 and 610 s were caused by reductions in the calculated condensation rate that occurred when a volume in the pressurizer model was filled. The slope change at 700 s was caused by the reinstatement of letdown flow when the SIAS was reset, resulting in a lower net inflow to the RCS.

Figure 18 shows a comparison of the hot leg temperatures. The trends and slopes of the calculated temperature agreed very well with the measured temperature. Again the temperature increased faster in the calculation than in the data after the pumps were tripped and the MSIVs closed.

The calculated and measured cold leg temperatures were in excellent agreement throughout the transient. The calculated temperature was very close to that shown in Figure 15.

The liquid levels from both steam generators are presented in Figure 19. The levels from the controlled pressure case are not shown because they remained off scale until nearly the end of the calculation. The calculated levels remained too low through most of the transient. A better calculation of the level in the A steam generator could have been achieved by allowing a slower main feedwater flow coastdown. The differences in the B steam generator level were probably caused by

differences in mass distribution in the steam generator between the plant and the calculation because of the excellent agreement in the calculation and data after 700 s. This agreement also indicated that the EFW flow to the B steam generator was close to that in the plant. The slope of the A steam generator level after 650 s again indicated that too much EFW was being injected. A separate calculation indicated that a reduction in the EFW flow to steam generator A of about 25% would have resulted in a good agreement between the calculated and measured slopes after 650 s.

The only difference between the lower pressurizer level calculation and the data that was not explained was the pressurizer pressure behavior between 160 and 210 s. Two phenomena were identified that could have caused the change to a slower depressurization rate in the data before the RCPs were tripped: higher head HPSI pumps, and voiding in the reactor vessel upper head. Calculations were performed that were identical to the lower pressurizer level calculation except for the HPSI pumps and the reactor vessel upper head temperature.

Figure 20 presents the pressurizer pressure from the data, the pressurizer level calculation, and from a calculation in which the HPSI began at a system pressure of 10.34 MPa (1500 psia) rather than 9.76 MPa (1415 psia). The trend of the data prior to the RCP trip was matched very well by the calculation. The depressurization rate slowed prior to the pump trip as the HPSI flow helped compensate the coolant shrink. The calculated behavior after the RCPs were tripped was similar to previous calculations.

Figure 21 presents the pressurizer pressure from the data, the pressurizer level calculation, and from a calculation in which the upper head fluid temperature was increased to 583 K (590°F). The calculated depressurization stopped when the saturation pressure of the liquid in the upper head was reached. The liquid flashed to steam, holding the pressure fairly constant until the RCPs were tripped. A more gradual change in the depressurization rate could have been achieved with a finer nodalization in the reactor vessel upper head, allowing a temperature distribution that would not have flashed large amounts of liquid at the same pressure.

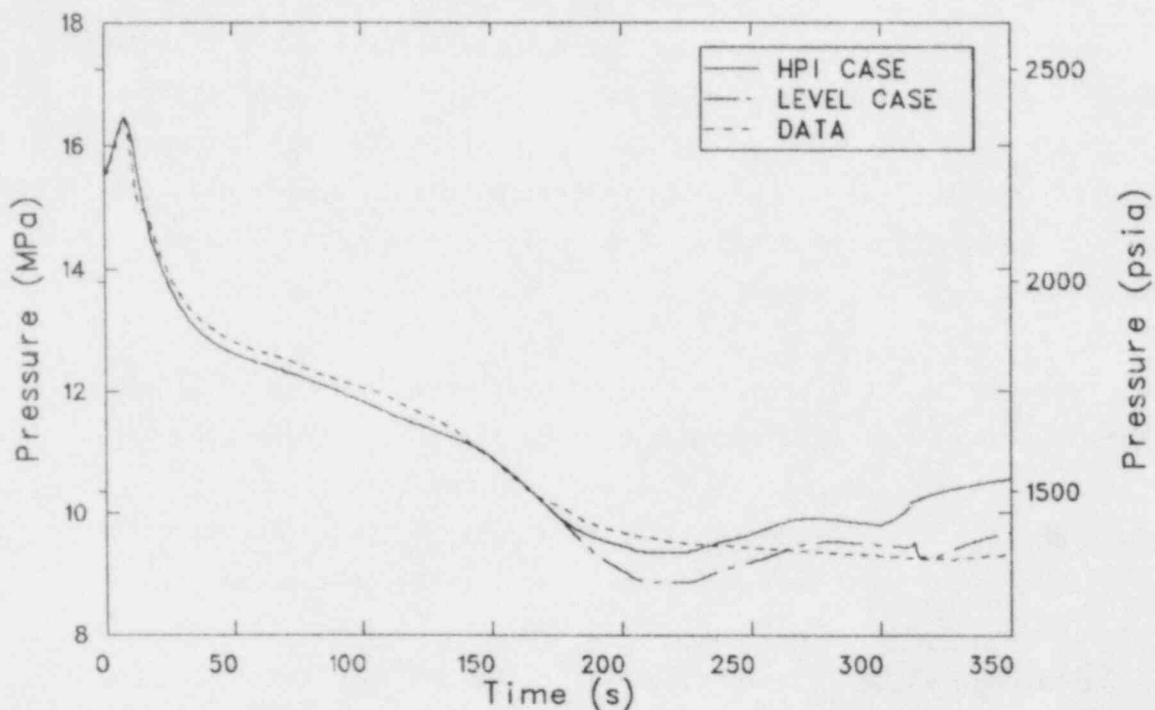


Figure 20. Pressurizer pressure from the higher pressure HPSI case, the pressurizer level case, and the data.

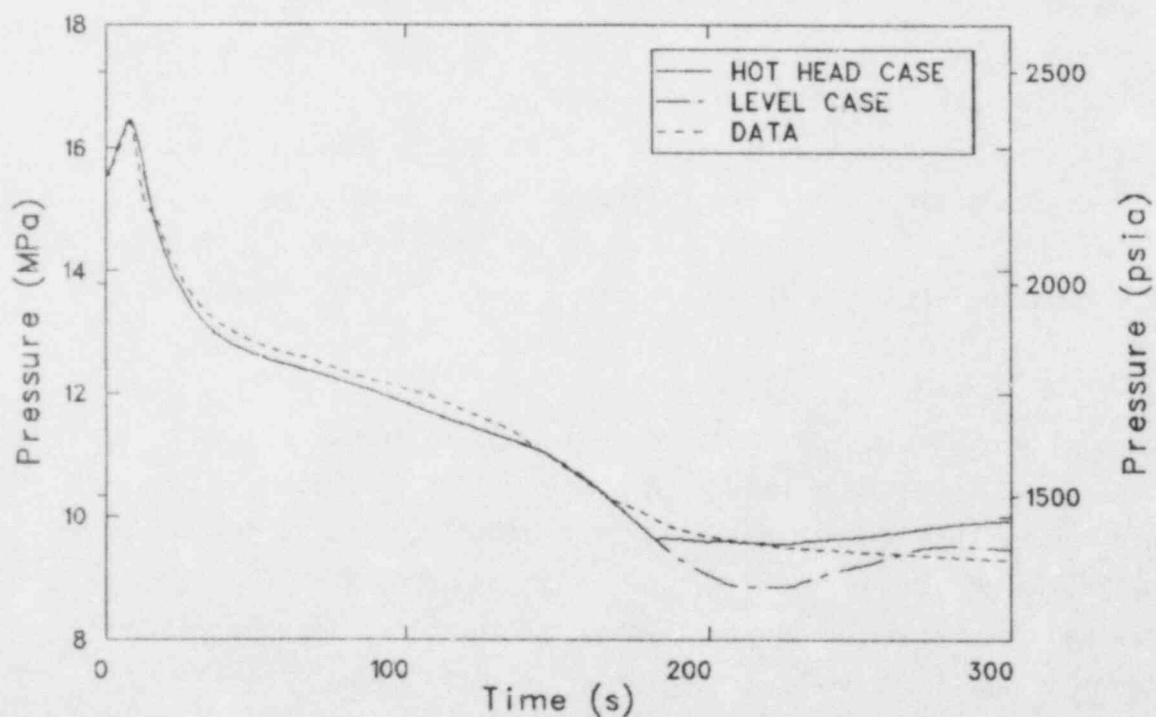


Figure 21. Pressurizer pressure from the hot upper head case, the pressurizer level case, and the data.

However, no information was available on temperatures in the upper head region to indicate whether voiding in the reactor vessel could have occurred during the transient or not.

From these two calculations, it was seen that using either higher head HPSI pumps or a higher upper head temperature in the calculations could account for the measured pressure behavior prior to the RCP trips.

3.2 Natural Circulation

Figure 22 shows the hot leg mass flow rate from the base and pressurizer level calculations. The RCPs were tripped between 200 and 204 s, and natural circulation was fully established by 650 s, when the pump head was negative. The flow coastdowns for the other calculations were nearly identical. The mass flow rate in the base calculation was about 5% higher than that in the pressurizer level calculation at 900 s. This flow difference was caused by the continued depressurization of the steam generators during the transient in the base calculation, which kept reducing the cold leg temperature. This caused a larger temperature difference between the hot and cold legs, which provided a larger driving force for the natural circulation flow.

The low flow rates existing during natural circulation were below the range of the plant flow instrumentation, so the temperature measurements were examined for flow indications.

Figure 23 presents the difference between the average hot and cold leg temperatures (loop ΔT) from the base calculation, the pressurizer level calculation, and the plant data. The loop ΔT decreased rapidly after the reactor scram. The calculated ΔT stayed fairly constant from 50 s until 200 s, when the RCPs were tripped. The measured ΔT increased slowly between 50 and 200 s. This increase may have been caused by a problem with the hot leg temperature measurements since the ΔT should have been constant. After the pumps were tripped, the increasing hot leg temperature caused by the flow reduction caused the calculated ΔT to increase and the measured ΔT to increase more rapidly. The loop ΔT decreased slightly

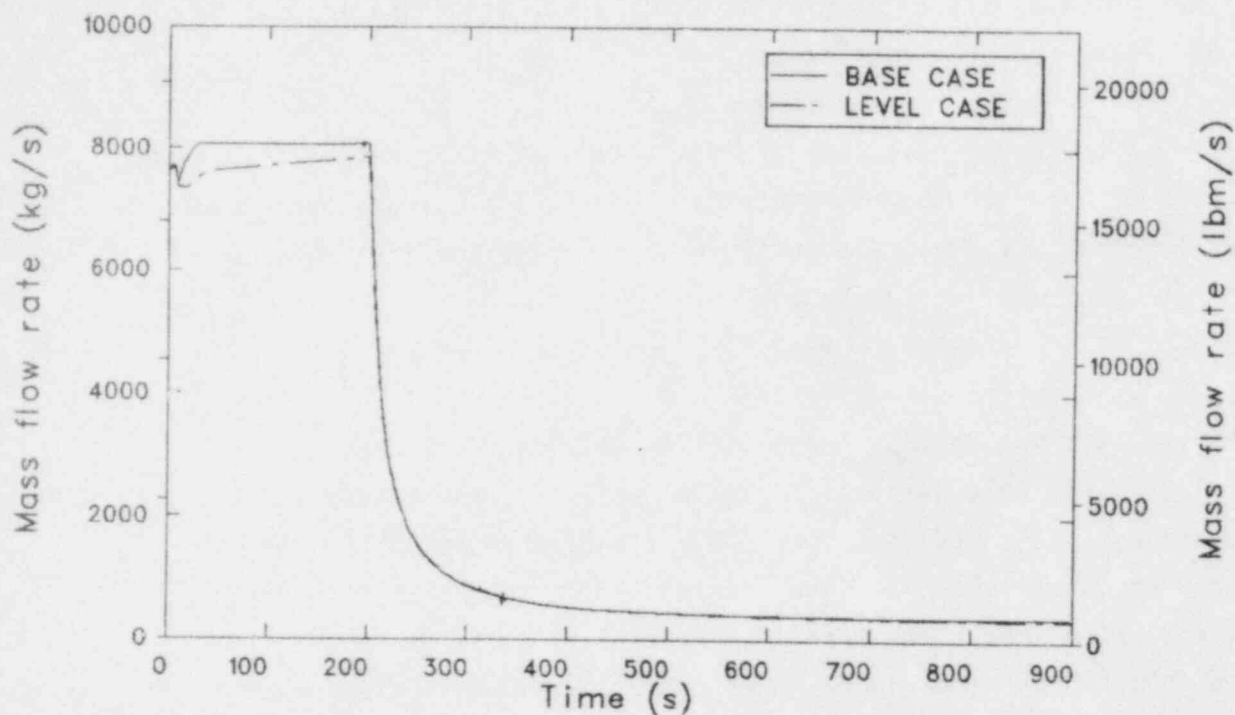


Figure 22. Hot leg mass flow rate from the base case and the pressurizer level case.

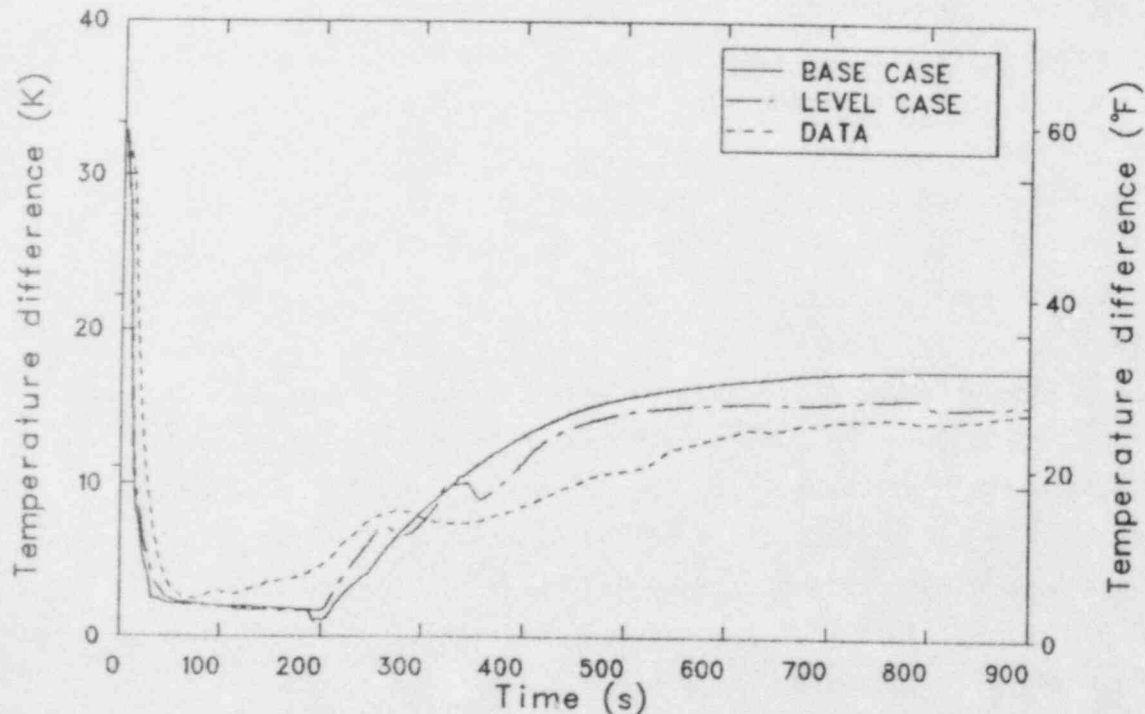


Figure 23. Loop temperature difference from the base case, the pressurizer level case, and the plant data.

before the pump trip in the base calculation because the closing of the MSIVs near 185 s caused an increase in the cold leg temperatures. The loop ΔT in the plant and the pressurizer level calculation decreased after the MSIVs closed at about 245 s as the cold leg temperatures increased, reflecting increases in the steam generator pressures and temperatures. As the warmer cold leg liquid passed through the core and reached the hot leg, the ΔT increased. The calculated ΔT in the pressurizer level case decreased again near 340 s when the A steam generator pressure began to increase. The calculated ΔT s were fairly steady by 650 s, when the flow coastdown was complete. The measured ΔT was fairly steady by about 700 s. The small drop in the loop ΔT in the pressurizer level calculation near 800 s was caused by a reduction in the charging flow, which increased the temperature at two of the cold leg measurement locations.

Another indication of the presence of flow was the coupling of the steam generator secondary temperature and the cold leg temperature. Figure 24 shows these temperatures for the A loop in the pressurizer level calculation. It can be seen that these temperatures were very close together after the reactor scram, during both forced and natural circulation flows. Figure 25 presents these temperatures from the measured data. Again, there was good agreement between the two through nearly all of the transient.

Although the coupling of the cold leg and steam generator temperatures was a good indication of loop flow, it was not possible to determine the presence of natural circulation using only these temperatures. The loop ΔT did provide an indication of the transition to and presence of natural circulation. The ΔT remained constant during forced circulation after the reactor scram, increased during the flow coastdown following the RCP trip, and remained constant during fully developed natural circulation. Transients in the steam generator pressures interrupted these trends, but only temporarily.

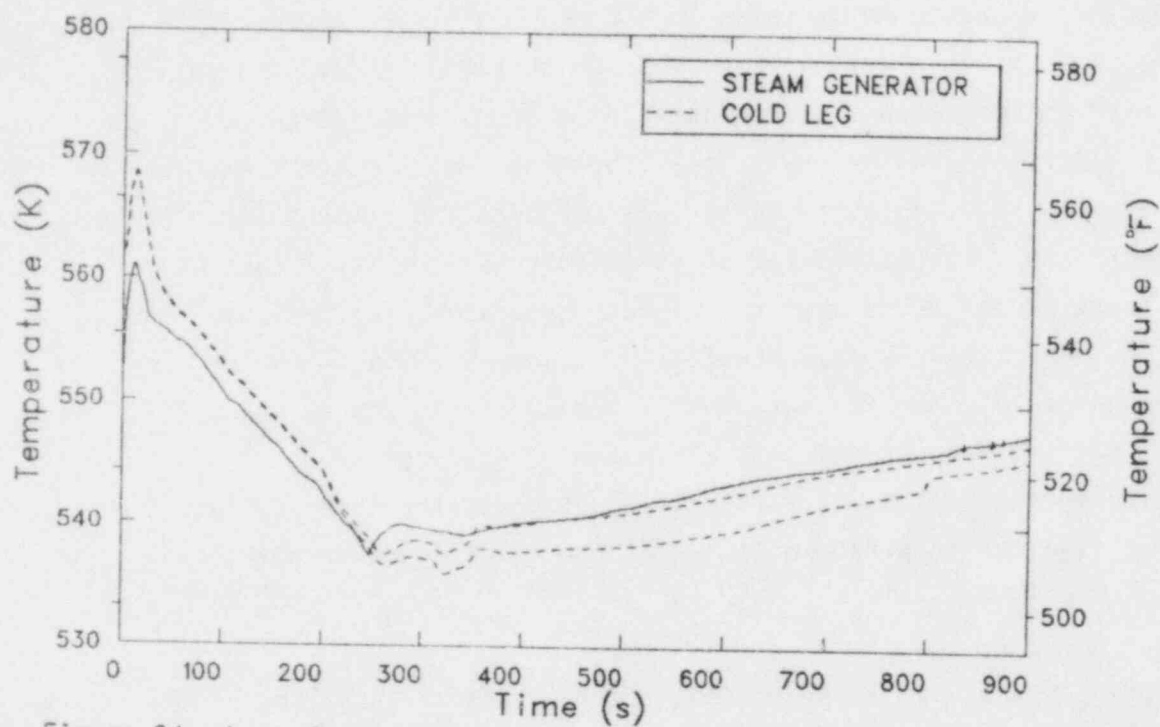


Figure 24. Loop A cold leg and steam generator temperatures from the pressurizer level case.

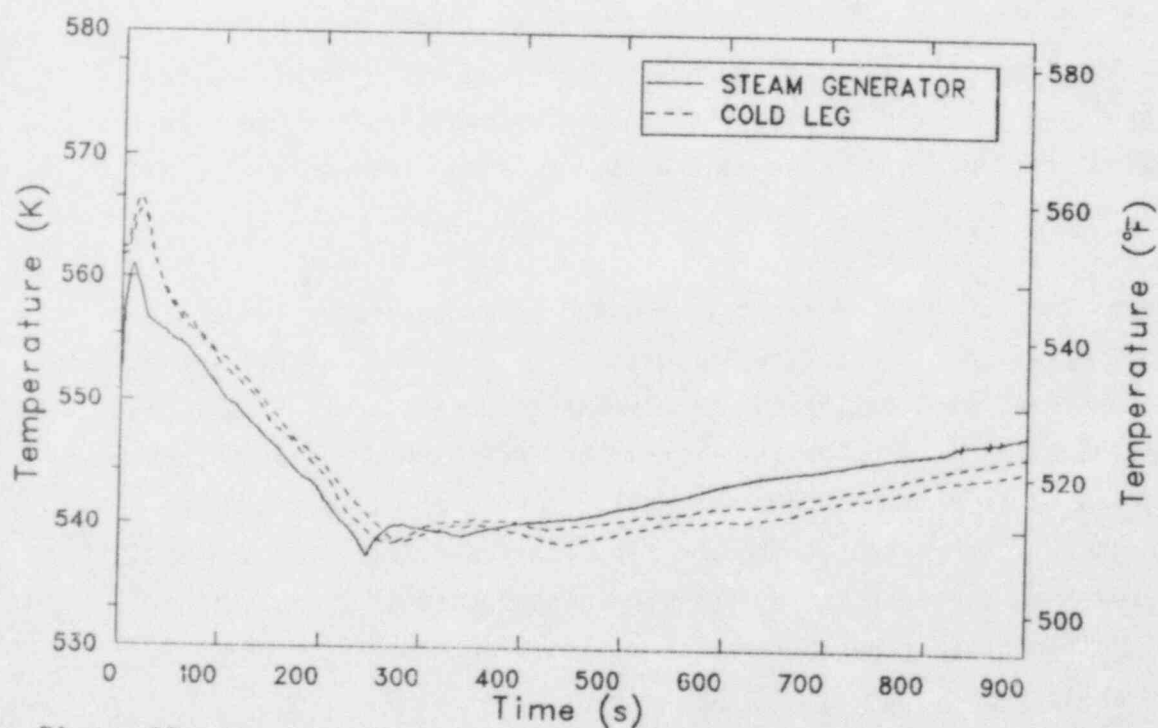


Figure 25. Loop A cold leg and steam generator temperatures from the plant data.

4. CONCLUSIONS

Conclusions based on the analysis of the January 29, 1980 turbine trip test at ANO-2 are presented below.

1. There were no major actions taken during the transient that were not reported in the transient descriptions.

The calculations were able to accurately reproduce the trends of the data. It did appear however, that the EFW flow to steam generator A was reduced by about 25% near 340 s. This action was seen in changes in the measured steam generator pressure and level.

2. Natural circulation was established in the plant and in all the calculations.

Natural circulation was fully established in the calculations 400-450 s after the RCPs were tripped. Plant temperature measurements indicated natural circulation was established at about the same time. The transition from forced to natural circulation was smooth.

3. The loop temperature measurements could be used to identify the presence of natural circulation.

The loop temperature difference was steady during forced circulation after the reactor scram, increased during the transition to natural circulation, and remained steady during fully developed natural circulation. These general trends can be temporarily interrupted by changes in secondary system pressure.

4. The reported initial pressurizer level may have been too high.

The initial pressurizer level has to be reduced from 49 to 35% in the calculations to reproduce the measured pressure response.

5. A change in the RCS depressurization rate prior to the RCP trip could have been caused by either the HPSI system or voiding in the the reactor vessel upper head.

The calculations showed that either HPSI at a slightly higher system pressure or higher temperatures in the upper head of the reactor vessel could have caused the observed responses.

However, sufficient information was not available to further identify the cause.

5. REFERENCES

1. V. H. Ransom et al., RELAP5/MOD1.5: Models, Developmental Assessment, and User Information, EGG-NSMD-6035, October 1982.
2. D. M. Kiser, Improved Steady State Edit/Testing Scheme for RELAP5, IS-NSMD-83-010, April 1983.
3. R. J. Wagner, RELAP5/MOD2 Shaft Control Component, IS-NSMD-83-014, April 1983.
4. J. A. Trapp, RELAP5/MOD2 Turbine Component Completion Report, IS-NSMD-83-015, April 1983.
5. D. M. Kiser, Improved Wall Drag Model for RELAP5/MOD2, IS-NSMD-83-016, April 1983.
6. J. A. Trapp, Cross-Flow Junction and Separator Upgrade Completion Report, IS-NSMD-83-019, April 1983.
7. J. C. Lin, R. A. Riemke, J. A. Trapp, RELAP5/MOD2 Hydrodynamic Numerical Scheme and Nonequilibrium Constitutive Models, IS-NSMD-83-021, April 1983.
8. J. C. Lin, Time Step Control for Heat Transfer, IS-NSMD-83-022, May 1983.
9. D. P. Siska, NSSS Transient Tests at ANO-2, EPRI NP-1708, May 1981.
10. P. D. Bayless, Analysis of the June 24, 1980 Loss of Off-Site Power Transient at Arkansas Nuclear One Unit 2, EGG-NTAP-6309, September 1983.
11. C. B. Davis, Analysis of the April 7, 1980 Loss of Off-Site Power Transient at Arkansas Nuclear One Unit 1 (Draft), EGG-SAAM-6381, August 1983.
12. T. R. Charlton ltr to P. E. Litteneker, "Transmittal of Preliminary Results of Natural Circulation Analyses for McGuire and North Anna," TRC-90-83, September 22, 1983.
13. P. A. Gagne, NSSS Design and Cycle 1 Operating History Data for Arkansas Nuclear One, Unit-2, EPRI NP-1707, March 1981.
14. T. W. Schnatz (Middle South Services) ltr to M. E. Waterman (EG&G Idaho), September 22, 1981.
15. Arkansas Power and Light Company, Arkansas Nuclear One, Unit 2, License Application FSAR, Docket No. 50368-63.
16. W. D. Lanning information transmittal to A. C. Peterson, October 1982.

NRC FORM 335 (11-81)		U.S. NUCLEAR REGULATORY COMMISSION BIBLIOGRAPHIC DATA SHEET		1. REPORT NUMBER (Assigned by DDC) EGG-SAAM-6415	
4. TITLE AND SUBTITLE ANALYSIS OF THE JANUARY 29, 1980 TURBINE TRIP AT ARKANSAS NUCLEAR ONE UNIT 2				2. (Leave blank)	
7. AUTHOR(S) P. D. Bayless				3. RECIPIENT'S ACCESSION NO.	
9. PERFORMING ORGANIZATION NAME AND MAILING ADDRESS (Include Zip Code) EG&G Idaho, Inc. Idaho Falls, ID 83415				5. DATE REPORT COMPLETED MONTH YEAR September 1983	
12. SPONSORING ORGANIZATION NAME AND MAILING ADDRESS (Include Zip Code) Office for Analysis and Evaluation of Operational Data U.S. Nuclear Regulatory Commission Washington, DC 20555				6. (Leave blank)	
13. TYPE OF REPORT Technical				DATE REPORT ISSUED MONTH YEAR September 1983	
15. SUPPLEMENTARY NOTES				8. (Leave blank)	
16. ABSTRACT (200 words or less) <p>The turbine trip that occurred at Arkansas Nuclear One Unit 2 on January 29, 1980 was analyzed using the RELAP5 computer code. The transient was investigated to understand the overall plant response, particularly in relation to natural circulation cooling. Sensitivity calculations were performed to explain the transient response. Methods of identifying the presence of natural circulation cooling were investigated.</p>				10. PROJECT/TASK/WORK UNIT NO.	
17. KEY WORDS AND DOCUMENT ANALYSIS				11. FIN NO. A6234	
17a. DESCRIPTORS				14. (Leave blank)	
17b. IDENTIFIERS: OPEN-ENDED TERMS				19. SECURITY CLASS (This report) Unclassified	
18. AVAILABILITY STATEMENT Unlimited				21. NO. OF PAGES	
20. SECURITY CLASS (This page) Unclassified				22. PRICE \$	